

## Magnetic and electronic properties in hole-doped manganese oxides with layered structures: $\text{La}_{1-x}\text{Sr}_{1+x}\text{MnO}_4$

Y. Moritomo, Y. Tomioka, A. Asamitsu, and Y. Tokura  
*Joint Research Center for Atom Technology, Tsukuba, Ibaraki 305, Japan*

Y. Matsui  
*National Institute for Research of Inorganic Materials, Tsukuba, Ibaraki 305, Japan*  
(Received 24 October 1994)

Electrical resistivity ( $\rho$ ) and magnetic susceptibility ( $\chi$ ) were measured for single crystals of  $\text{La}_{1-x}\text{Sr}_{1+x}\text{MnO}_4$  ( $0.0 \leq x \leq 0.7$ ), which were grown by the floating-zone method with varying the nominal hole concentration ( $x$ ). With hole doping, critical temperature ( $T_N$ ) for the antiferromagnetic phase transition decreases and eventually a spin-glass phase appears for  $x \geq 0.2$ , perhaps due to the competition between the generic antiferromagnetic superexchange interaction and the ferromagnetic double-exchange interaction. At  $x \approx \frac{1}{2}$ , real-space ordering of the doped holes occurs at  $\sim 220$  K, accompanying a steep increase of  $\rho$  as well as a suppression of  $\chi$ .

Extensive studies on the normal-state properties in cuprate superconductors have aroused extended interest in the correlated dynamics of spins and charges in perovskite transition-metal oxides with  $3d$  electrons. Among a number of barely metallic  $3d$  electron systems, hole-doped manganese oxides with perovskite structure, e.g.,  $\text{La}_{1-x}\text{Sr}_x\text{MnO}_3$ , are known to be conducting ferromagnets,<sup>1,2</sup> in which the magnetic interaction is mediated by the transfer of the holes (the so-called double-exchange interaction).<sup>3-6</sup> Large negative magnetoresistance effects have been reported around the magnetic phase transition temperature for these manganese oxides, e.g.,  $\text{La}_{1-x}\text{Pb}_x\text{MnO}_3$  ( $x=0.31$ ),<sup>7</sup>  $\text{Nd}_{1-x}\text{Pb}_x\text{MnO}_3$  ( $x=0.5$ ),<sup>8</sup> and  $\text{La}_{1-x}\text{Sr}_x\text{MnO}_3$  ( $x=0.1-0.4$ ),<sup>9</sup> which begins to attract current interest in relation to possible application of the giant magnetoresistance (GMR). In this paper, we will report on electronic and magnetic properties for hole-doped manganese oxides with layered perovskite structures ( $\text{K}_2\text{NiF}_4$  structure), single crystals of  $\text{La}_{1-x}\text{Sr}_{1+x}\text{MnO}_4$ , and deduce the electronic phase diagram as a function of the nominal hole concentration ( $x$ ). The nominally hole-undoped compound  $\text{LaSrMnO}_4$  ( $x=0.0$ ) is known to be an antiferromagnet.<sup>10</sup> In the solid solution, we can control the effective Mn valence from  $3+$  ( $x=0.0$ ) to  $4+$  ( $x=1.0$ ), without changing the two-dimensional Mn-O-Mn network.

Confinement of the Mn-O-Mn network in two dimensions ( $\text{MnO}_2$  sheet) should reduce the one-electron  $3d$ -band width as compared with the perovskite compounds with three-dimensional network. Especially in  $\text{La}_{1-x}\text{Sr}_{1+x}\text{MnO}_4$ , carrier holes may have a large component of the  $d_{3z^2-r^2}$  orbital, which extends perpendicular to the  $\text{MnO}_2$  sheet. The resultant decrease of itineracy of the holes weakens the double-exchange interaction, which may be inferior to the antiferromagnetic interaction. It is also possible that repulsive Coulomb interaction between the less itinerant holes induces some real-space ordering, analogously to the Verwey transition observed in magnetite  $\text{Fe}_3\text{O}_4$ .<sup>11</sup> Recently, ordering of the doped holes has been reported for nickel oxides with layered perovskite structure,  $\text{La}_{2-x}\text{Sr}_x\text{NiO}_4$ , at  $x \approx \frac{1}{3}$  and  $x \approx \frac{1}{2}$ .<sup>12</sup>

Pioneering work has been done by Rao *et al.* for ceramic samples of  $\text{La}_{1-x}\text{Sr}_{1+x}\text{MnO}_4$  ( $0.25 \leq x \leq 0.75$ ):<sup>13</sup> Their results show the absence of the ferromagnetic transition in this  $x$  range. We have grown single crystals of  $\text{La}_{1-x}\text{Sr}_{1+x}\text{MnO}_4$  over the composition range of  $0.0 \leq x \leq 0.7$  and carefully investigated the change in magnetic and electronic properties as well as their anisotropy. With hole doping, we observed the disappearance of the antiferromagnetic (AF) phase transition and the subsequent emergence of the spin-glass (SG) phase for  $x \geq 0.2$ . Furthermore, we observed real-space ordering of the doped holes for  $x=0.5$  and resultant anomalies in magnetic and electronic properties.

Single-crystalline samples of  $\text{La}_{1-x}\text{Sr}_{1+x}\text{MnO}_4$  ( $0.0 \leq x \leq 0.7$ ) were melt-grown by the floating-zone method at a feeding speed of 10–20 mm/h. First, a stoichiometric mixture of  $\text{La}_2\text{O}_3$ ,  $\text{SrCO}_3$ , and  $\text{Mn}_3\text{O}_4$  was ground and calcined three times at 1250–1350 °C for 10–30 h. Then, the obtained powder was pressed into a rod with a size of 5 mm  $\phi \times 60$  mm and sintered at 1450 °C for 12 h. Over the whole concentration range, the ingredient could be melted congruently. The nominally hole-undoped compound  $\text{LaSrMnO}_4$  ( $x=0.0$ ) was grown in a flow of Ar (6N purity). Other crystals were grown in an oxygenating atmosphere with controlled  $\text{O}_2$  gas pressure: in a flow of air for  $x=0.1$ , in a flow of  $\text{O}_2$  for  $x=0.2-0.4$ , 2 atm of  $\text{O}_2$  for  $x=0.5$ , 3 atm of  $\text{O}_2$  for  $x=0.6$ , and 5 atm of  $\text{O}_2$  for  $x=0.7$ . The obtained crystals are easily cleaved along the  $c$  face, which is parallel to the growth direction. To characterize the crystals, x-ray-diffraction measurement as well as electron probe microanalysis (EPMA) were carried out. The results indicate that all the crystals are single phase and show nearly identical composition with the prescribed one. The crystal symmetry is tetragonal ( $I4/mmm$ : the so-called  $\text{K}_2\text{NiF}_4$  structure) over the whole composition range. The  $c$  axis significantly decreases with  $x$  from 13.17 Å ( $x=0.0$ ) to 12.40 Å ( $x=0.6-0.7$ ), while the  $a$  axis is nearly independent of  $x$  (3.80–3.86 Å). The obtained lattice parameters agree with the data reported for the ceramic samples.<sup>13,14</sup>

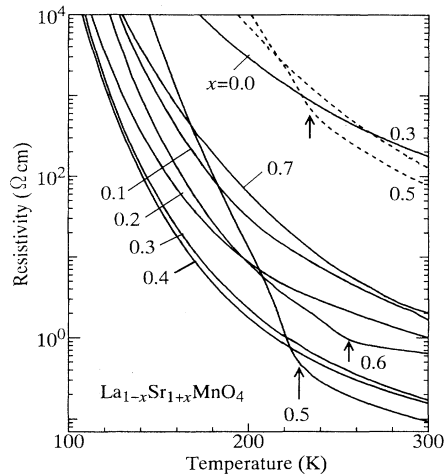


FIG. 1. Temperature dependence of resistivity ( $\rho$ ) for single crystals of  $\text{La}_{1-x}\text{Sr}_{1+x}\text{MnO}_4$  with various hole concentrations ( $x$ ). Solid and broken curves stand for the in-plane ( $\rho_{ab}$ ) and the out-of-plane ( $\rho_c$ ) components, respectively. A steep increase in  $\rho$  is observed at a specific temperature ( $T_V$ ) for  $x=0.5$  and  $0.6$ , as indicated by upward arrows.

First, we show in Fig. 1 temperature dependence of resistivity ( $\rho$ ) for  $\text{La}_{1-x}\text{Sr}_{1+x}\text{MnO}_4$  with varying  $x$  value: Solid and broken curves are for the in-plane ( $\rho_{ab}$ ) and the out-of-plane ( $\rho_c$ ) components, respectively. For four-probe resistivity measurements, the sample was cut into a rectangular shape, typically  $3 \times 2 \times 1 \text{ mm}^3$ , and electrical contacts were made with silver paste. The parent compound  $\text{LaSrMnO}_4$  ( $x=0.0$ ) shows an insulating behavior with a thermal activation energy of  $\sim 70 \text{ meV}$ . A hole-doping procedure by substitution of the La sites with Sr considerably reduces  $\rho_{ab}$ , yet the system remains insulating or semiconducting. Motion of the doped holes appears to be highly anisotropic: For  $x=0.3$ ,  $\rho_c$  (dotted curve) is  $\sim 10^3$  times as large as  $\rho_{ab}$ . With further increasing  $x$ ,  $\rho_{ab}$  rather increases (see the  $x=0.6$  and  $0.7$  data in Fig. 1).

It is worth noting that  $\rho_{ab}$  and  $\rho_c$  for the  $x=0.5$  sample steeply increases at  $\sim 220 \text{ K}$  (upward arrows in Fig. 1). Hereafter,  $T_V$  is defined as the temperature at which the  $\rho$ - $T$  curve shows a steep increase. A similar rise of  $\rho_{ab}$  is also observed for  $x=0.6$  at  $T_V \sim 250 \text{ K}$  (upward arrow), while the anomaly appears to be absent for  $x=0.7$ . Absence of the thermal hysteresis in the resistivity change implies a second-order phase transition at  $T_V$ . In accord with these anomalies in  $\rho$ , magnetic susceptibility ( $\chi$ ) for  $x=0.5$  and  $0.6$  also shows a singular behavior: The Curie-Weiss-like increase of  $\chi$  in the high-temperature region ( $\geq 300 \text{ K}$ ) begins to be suppressed at around  $T_V$  (see arrows in Fig. 2). (Note that enhancement of  $\chi$  below  $\sim 100 \text{ K}$  is a precursor of the SG transition, as argued later.)

The transition at  $T_V$  is considered to be characterized as a change in the electronic structure, rather than as a simple structure change, because the singularities are observed in the restricted  $x$  region ( $x=0.5$ – $0.6$ ), where no anomalous behavior is observed in the room-temperature lattice parameters. It is likely that at  $x \approx \frac{1}{2}$  the holes produced on the  $\text{MnO}_2$  sheets show a periodic arrangement on every other

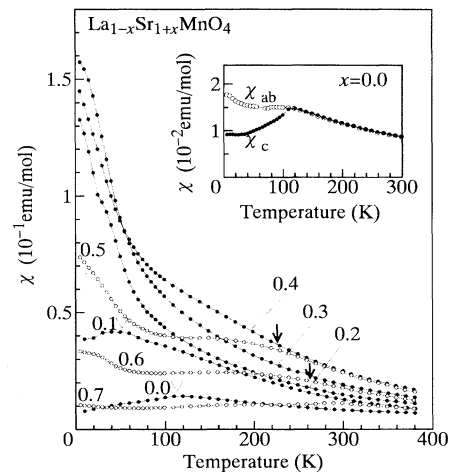


FIG. 2. Temperature dependence of susceptibility ( $\chi$ ;  $H \parallel c$ ) for single crystals of  $\text{La}_{1-x}\text{Sr}_{1+x}\text{MnO}_4$  measured with a field of  $1 \text{ T}$  after cooling down to  $5 \text{ K}$  in the field. Open triangles stand for the antiferromagnetic transition. The Curie-Weiss-like increase of  $\chi_c$  appears to be suppressed for  $x=0.5$  and  $0.6$ , as indicated by downward arrows. The inset shows the anisotropy of  $\chi$  for  $\text{LaSrMnO}_4$  ( $x=0.0$ ) measured with a field of  $10 \text{ mT}$ : Open and closed circles are for the in-plane ( $\chi_{ab}$ ) and the out-of-plane ( $\chi_c$ ) components, respectively.

Mn site via the repulsive Coulomb interaction between them. Hereafter, we call such a periodic arrangement of the holes charge ordering (CO) state. In such a CO state, charge density would be modulated with twofold periodicity along the  $[110]$  and  $[1\bar{1}0]$  directions (i.e., along the diagonal of the  $\text{MnO}_2$  square lattice), accompanied by the lattice modulation. Figure 3 shows  $[001]$  zone-axis electron diffraction patterns obtained at (a)  $300 \text{ K}$  ( $> T_V$ ) and (b)  $110 \text{ K}$  ( $< T_V$ ) for  $\text{La}_{0.5}\text{Sr}_{1.5}\text{MnO}_4$  ( $x=0.5$ ). A striking feature is the appearance of sharp superlattice spots below  $T_V$  [see Fig. 3(b)], which indicates a modulation parallel to the  $[110]$  (or  $[1\bar{1}0]$ ) direction. The observed fourfold modulation rather than the expected twofold one may be due to the extra lattice modulation induced by the ordering of the holes. Two series of the spots along the  $[110]$  and  $[1\bar{1}0]$  directions are likely to come from different areas of the twinned sample, judging from the absence of the second harmonics like  $(\frac{1}{2}, 0, 0)$ . Charge transport as well as magnetic susceptibility are considerably affected in the CO state, as observed. This is because transfer of a hole to the neighboring site is disturbed by the electrostatic potential produced by the ordered holes, which results in an increase of  $\rho$  as well as a suppression of  $\chi$ . Similar effects of the CO transition on the  $\rho$ - $T$  and  $\chi$ - $T$  curves are observed in ceramic samples of  $\text{La}_{2-x}\text{Sr}_x\text{NiO}_4$  at  $x \approx \frac{1}{3}$ .<sup>12</sup>

Now, let us proceed to magnetic properties of  $\text{La}_{1-x}\text{Sr}_{1+x}\text{MnO}_4$ . The temperature dependence of magnetization ( $M$ ) was measured under various magnetic fields ( $H$ ) up to  $1 \text{ T}$  using a superconducting quantum interference device magnetometer.<sup>15</sup> Apart from the lower temperature region ( $\leq 150 \text{ K}$ ), where the spin-glass phase (*vide infra*) set in,  $M$  is proportional to  $H$ . We show in Fig. 2 the temperature variation of the magnetic susceptibility ( $\chi \equiv M/H$ ) mea-

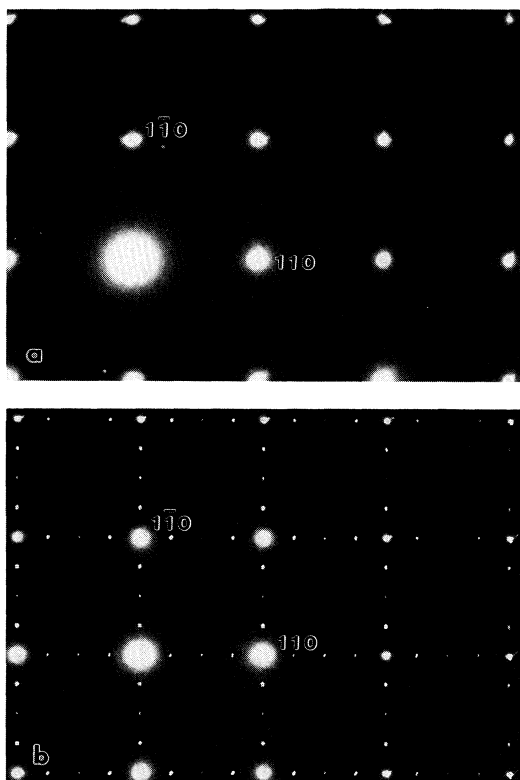


FIG. 3. [001] zone-axis electron diffraction patterns observed at (a) 300 K and (b) 110 K for  $\text{La}_{0.5}\text{Sr}_{1.5}\text{MnO}_4$  ( $x=0.5$ ). Fundamental diffraction spots are indexed with a tetragonal cell ( $a=b=3.57$  Å,  $c=12.49$  Å). The presence of superlattice spots is evident at 110 K (lower figure).

sured with a magnetic field of 1 T applied parallel to the  $c$  axis after cooling down to 5 K in the field (FC). The  $\chi$ - $T$  curves for  $0.4 \leq x \leq 0.7$  qualitatively agree with the previously reported data for ceramic samples.<sup>13</sup> The inset shows anisotropy of  $\chi$  for  $\text{LaSrMnO}_4$  ( $x=0.0$ ) measured with a field of 10 mT: Open and closed circles are for the in-plane ( $\chi_{ab}$ ) and the out-of-plane ( $\chi_c$ ) components, respectively. With decreasing temperature,  $\chi_c$  shows a cusp at  $T_N \sim 120$  K and then decreases, while  $\chi_{ab}$  becomes nearly temperature independent below  $T_N$ . These behaviors are characteristic of an antiferromagnetic (AF) phase transition with spins aligned along the  $c$  axis, which is consistent with the spin structure derived from the neutron diffraction.<sup>10</sup>  $T_N$  (open triangles) decreases with hole doping and vanishes for  $x \geq 0.2$ . In the high-temperature region ( $\geq 300$  K), the  $\chi$ - $T$  curves approximately obey the Curie-Weiss law. The estimated Curie temperature is positive (60–110 K) for  $0.2 \leq x \leq 0.6$ , implying the ferromagnetic interaction mediated by the double-exchange mechanism.

The spin-glass (SG) phase shows up in between  $x=0.2$  and 0.6, perhaps due to the competition between the ferromagnetic double-exchange interaction and the antiferromagnetic superexchange interaction. We show in Fig. 4 a typical example of temperature variation of  $M$ : (a) the out-of-plane ( $H \parallel c$ ) and (b) the in-plane ( $H \perp c$ ) component for  $x=0.3$ . The  $M$  value was measured with a field of 1 mT after cool-

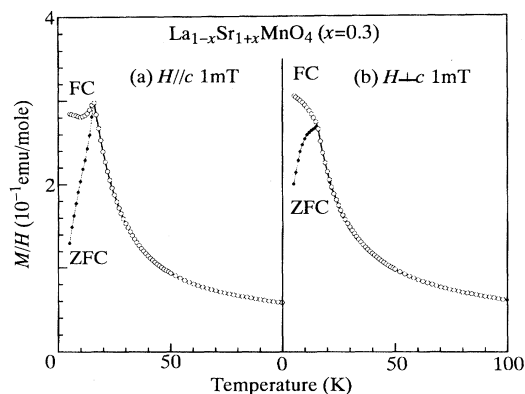


FIG. 4. Temperature dependence of magnetization ( $M$ ) for  $\text{La}_{0.7}\text{Sr}_{1.3}\text{MnO}_4$  ( $x=0.3$ ) measured with a field of 1 mT after cooling down to 5 K in the field (FC: open circles) and in the zero field (ZFC: closed circle): (a) the out-of-plane and (b) the in-plane components.

ing down to 5 K in the field (FC; open circles) or in the zero field (ZFC; close circles). The ZFC curve of the out-of-plane component [closed circles in Fig. 4(a)] critically increases on approaching  $T_g \sim 16$  K from the high-temperature side and then decreases showing a cusp structure. Below  $T_g$ , the FC curve (open circles) starts to deviate from the ZFC curve. These features, which are also seen in the in-plane component [Fig. 4(b)], are characteristic of a SG transition.<sup>16</sup> Similar SG transitions are observed at  $T_g \sim 25$  K for  $x=0.2, 0.4$ , and 0.6 and  $\sim 20$  K for  $x=0.5$ .

To summarize, thus obtained transition temperatures for  $\text{La}_{1-x}\text{Sr}_{1+x}\text{MnO}_4$ , i.e.,  $T_N$  (AF transition),  $T_g$  (SG transition), and  $T_V$  (CO transition), are plotted in the lower panel of Fig. 5. We also plot the values of dc conductivity ( $\sigma_{ab}$ ) and susceptibility ( $\chi_c$ ) at 150 K in the upper panel, to see  $x$ -dependent kinetics of the doped holes. These quantities,

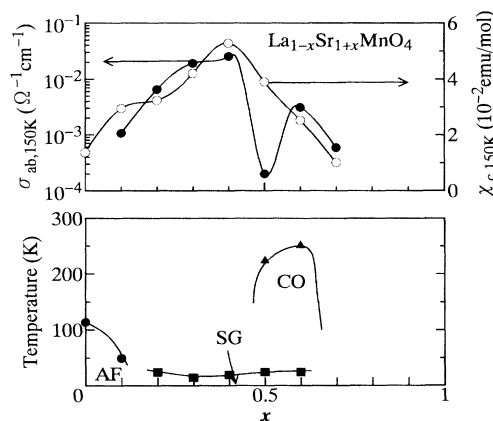


FIG. 5. Upper panel: Hole concentration ( $x$ ) dependence of dc conductivity ( $\rho_{ab}$ ; closed circles) and magnetic susceptibility ( $\chi_c$ ; open circles) at 150 K for  $\text{La}_{1-x}\text{Sr}_{1+x}\text{MnO}_4$ . Lower panel: Electronic phase diagram for  $\text{La}_{1-x}\text{Sr}_{1+x}\text{MnO}_4$ . AF, SG, and CO stand for the antiferromagnetic, spin-glass, and charge-ordering phases, respectively. Solid lines are merely a guide to the eye.

i.e.,  $\sigma_{ab,150\text{ K}}$  and  $\chi_{c,150\text{ K}}$ , are crude measures for the magnitude of itineracy of the holes and the ferromagnetic interaction, which are least affected by the SG phase present at lower temperature ( $\leq 25\text{ K}$ ). Both values increase with  $x$  up to  $x=0.4$ , indicating that the double-exchange interaction increases with a gain in kinetic energy of the holes. Such a ferromagnetic interaction appears to induce the SG transition in competition with the generic antiferromagnetic superexchange interaction. The sudden reduction of these quantities

at  $x \approx 0.5$  obviously reflects an occurrence of the real-space ordering of the holes (CO state). Thus, hole doping on the layered perovskite manganese oxide produces the exceedingly rich feature due to the correlated dynamics of spins and charges.

The authors are grateful to T. Arima for his help and kind advice during the crystal growth work. This work was supported by New Energy and Industrial Technology Development Organization (NEDO), Japan.

- 
- <sup>1</sup>G. H. Jonker and J. H. Santen, *Physics* **16**, 337 (1950).  
<sup>2</sup>E. O. Wollan and W. C. Koehler, *Phys. Rev.* **100**, 548 (1955).  
<sup>3</sup>C. Zener, *Phys. Rev.* **82**, 403 (1951).  
<sup>4</sup>P. W. Anderson and H. Hasegawa, *Phys. Rev.* **100**, 675 (1955).  
<sup>5</sup>P.-G. de Gennes, *Phys. Rev.* **118**, 141 (1960).  
<sup>6</sup>K. Kubo and N. Ohata, *J. Phys. Soc. Jpn.* **33**, 21 (1972).  
<sup>7</sup>C. W. Searle and S. T. Wang, *Can. J. Phys.* **47**, 2703 (1969).  
<sup>8</sup>R. M. Kusters, J. Singleton, D. A. Keen, R. McGreevy, and W. Hayes, *Physica B* **155**, 362 (1989).  
<sup>9</sup>Y. Tokura, A. Urushibara, Y. Moritomo, T. Arima, A. Asamitsu, G. Kido, and N. Furukawa, *J. Phys. Soc. Jpn.* **63**, 3931 (1994).  
<sup>10</sup>S. Kawano, N. Achiwa, N. Kamegashira, and M. Aoki, *J. Phys. (Paris) Colloq.* **49**, C8-829 (1988).  
<sup>11</sup>E. J. W. Verwey and P. W. Haaymann, *Physica* **8**, 979 (1941).  
<sup>12</sup>C. H. Chen, S.-W. Cheong, and A. S. Cooper, *Phys. Rev. Lett.* **68**, 345 (1993); S.-W. Cheong, H. Y. Hwang, C. H. Chen, B. Batlogg, L. W. Rupp, Jr., and S. A. Carter, *Phys. Rev. B* **49**, 7088 (1994).  
<sup>13</sup>C. N. R. Rao, P. Ganguly, K. K. Singh, and R. A. Mohan Ram, *J. Solid State Chem.* **72**, 14 (1988); M. A. Mohan Ram, P. Ganguly, and C. N. R. Rao, *ibid.* **70**, 82 (1987).  
<sup>14</sup>P. Ganguly and C. N. R. Rao, *J. Solid State Chem.* **53**, 193 (1984).  
<sup>15</sup>The  $M$ - $T$  curves measured with low magnetic fields are deformed for  $x=0.1$  and  $0.2$ , possibly due to intergrowth of a ferromagnetic phase such as  $(\text{La,Sr})\text{MnO}_3$ , although no trace of the impurity phase was detectable in the powder x-ray diffraction patterns.  
<sup>16</sup>For example, see K. Binder and A. P. Young, *Rev. Mod. Phys.* **58**, 801 (1986).

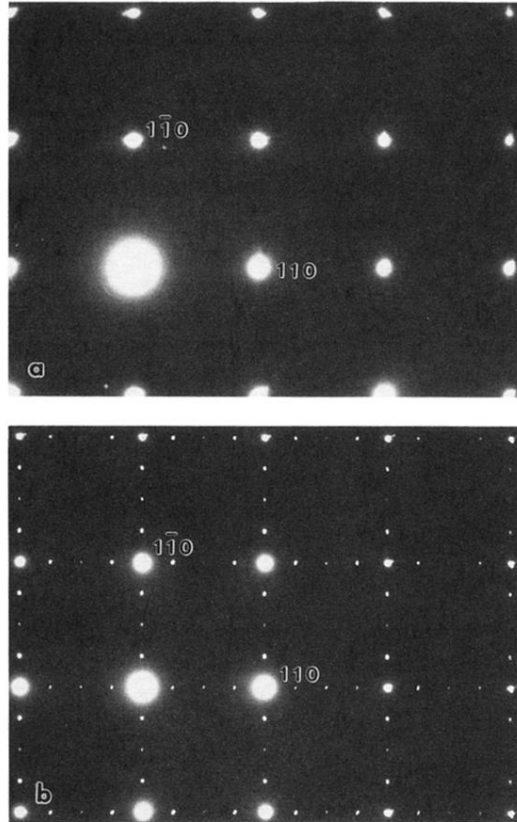


FIG. 3. [001] zone-axis electron diffraction patterns observed at (a) 300 K and (b) 110 K for  $\text{La}_{0.5}\text{Sr}_{1.5}\text{MnO}_4$  ( $x=0.5$ ). Fundamental diffraction spots are indexed with a tetragonal cell ( $a=b=3.57 \text{ \AA}$ ,  $c=12.49 \text{ \AA}$ ). The presence of superlattice spots is evident at 110 K (lower figure).